



“HENRI COANDA”
AIR FORCE ACADEMY
ROMANIA



“GENERAL M.R. STEFANIK”
ARMED FORCES ACADEMY
SLOVAK REPUBLIC

INTERNATIONAL CONFERENCE of SCIENTIFIC PAPER
AFASES 2015
Brasov, 28-30 May 2015

EFFECT OF LIGHT DEPENDANT RESISTOR MISMATCHING AND IMPACT OF NON LINEARITY IN A SMALL SCALE SOLAR TRACKING SYSTEM

Philippe Dondon*, Ecaterina-Liliana Miron**

*Université de Bordeaux, IPB, Talence, France, **Faculty of Aeronautical Management, “Henri Coandă”
Air Force Academy, Brasov, Romania

Abstract: *The design of a didactical small scale “green” house and its power production systems has been previously presented in [1]. As power generation is one of the challenges in Sustainable Development, some scaled accessories have been included on house surroundings. In particular, a small scale simplified solar tracking analogue system based on LDR sensors, has been designed and installed [2]. A mixed SPICE modelling of the system, including geometrical, optical, electronic linear and nonlinear aspects has been built. This new paper focuses on effects of Light Dependant Resistor mismatching, and impact of non-linearity on the solar tracking performances. Firstly, the principle of tracking and its SPICE modelling are shortly described; Secondly, impacts of each imperfection are detailed and simulated. Finally, impacts are quantified and discussed before conclusion.*

Key words: *Sun tracking, Mixed SPICE modelling, Analogue design, Sustainable development*

1. INTRODUCTION

1.1 Small scale house project state of art.

Within the framework of an innovative sustainable development project, the design a functional realistic small scale house, built in genuine materials took almost three years. The building (with true materials) of small scale house itself is finished. It required more than 1500 hours of work and was detailed in [1]. Figure 1 shows a picture of the finished small scale model (at 1/20 scale).

The small scale model will be used as:

- Demonstrator (sustainable development exhibition in town halls or local sustainable development events)

- Pedagogical support for practical lessons and electronic projects, for sensitizing engineering students to green power management, power saving and low power electronic in first and 2nd year study

1.2 Study background. We designed several electronic boards and their electronic control circuits, as indicated hereafter, in order to make the “green” house model, didactical and fully functional:

- A small scale home automation including weather station, low voltage LED lighting for the terrace, roof solar panel and battery cells management, “air conditioned” system powered by an hydrogen fuel stack (i.e. scaled Canadian well under the house), an electrical

heater circuit house and its temperature control.

- A solar tower and its performance measurement system,
- A small scale simplified solar tracking system for a solar panel...



Figure 1: View of house and surroundings.

The present paper focuses on intrinsic imperfection of this last accessory. Modelling and design has already been detailed [2]. However, effects of mismatching and other imperfection must be taken in consideration for a fine analysis of the system's behavior. For a better understanding, we bring back to mind in §2. and §3. some important points.

2. SUN TRACKING CIRCUIT PRINCIPLE

2.1 Generalities. The didactical designed circuit is obviously a simplified version of a true system [3], [4], [5]. Main goals were to illustrate feedback theory taught in our electronic engineering school and more generally to introduce sustainable development in scientific studies.

2.2 Principles and schematic. The small scale "green house" is used for in-door demonstration and applications. Thus, a halogen spot light is used to "replace" the sun light.

The system consists of an analogue system with one rotation axis control (horizontal plan) [6], [7] to simplify the approach. Figure 2 shows the sun tracking principle.

When the solar panel is aligned in "sun" direction, the received left and right lights flux $L1$ and $L2$ are equal (Cf. figure 3). When it is

not, one of the two LDR receives more flux than the other. This generates an analogue difference voltage V_{diff} ("left minus right") and the feedback loop moves the servo motor into the right direction until to cancel the voltage V_{diff} .

A classical hobbyist servo Futaba (or equivalent) is used to move the panel. According to standards, the rotation angle α is proportional to an input control signal V_{pwm} with the following characteristics: two voltage level signal 0, +5V, period 20ms, pulse width variable from 1ms to 2ms for a 0° to 180° rotation. Thus, a DC to PWM converter is required between subtraction block and Servo input (Cf. figure 2).

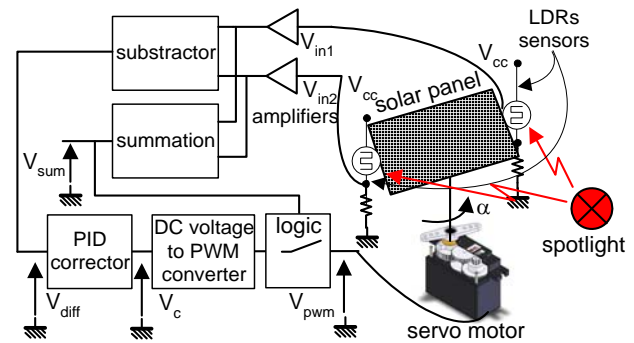


Figure 2: Sun tracking system block diagram

Two light sensors LDR1 and LDR2 (LDR: Light Dependant Resistors,) are located on left and right side of the panel. They receive the "sun" light.

A summation V_{sum} of the two sensors voltages is used to distinguish dark and sunny situation; and power consumption is minimized during the "night" by turning off the servo voltage supply.

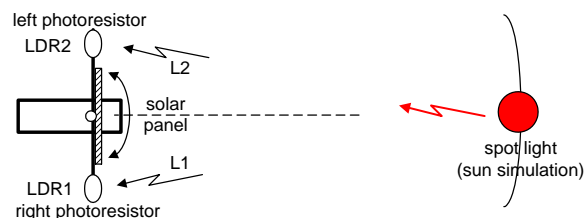


Figure 3: Solar panel alignment



"HENRI COANDA"
AIR FORCE ACADEMY
ROMANIA



"GENERAL M.R. STEFANIK"
ARMED FORCES ACADEMY
SLOVAK REPUBLIC

INTERNATIONAL CONFERENCE of SCIENTIFIC PAPER
AFASES 2015
Brasov, 28-30 May 2015

3. MODELLING OF TRACKING SYSTEM

3.1 Generalities. L_1 , L_2 represents the received light (in Lux) on each LDR, α_{ref} the "sun" angular position, α_e the error angle, α the angle given by the servo motor (referenced as indicated in figure 5). Thus, the tracking system can be modelled as follow:

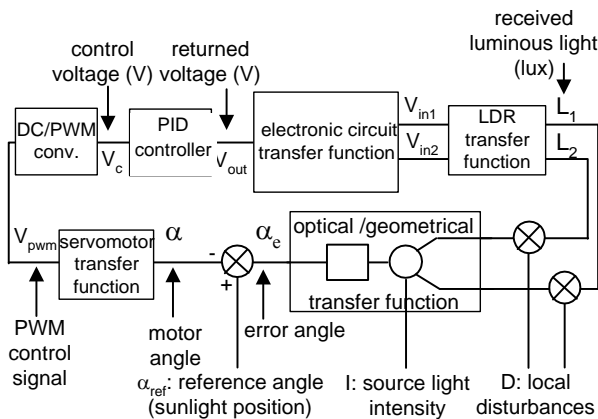


Figure 4: System identification

- α_{ref} is the main input of the feedback system.
- Source light intensity input (I) can be seen as a parasitic input which represents fluctuation of source intensity (fog, sky partially cloudy, etc).
- Local disturbances input (D) represent disturbances that can occur individually, on each LDR optical way. (object passing over the LDR etc).

We set up:

$$L_0 = I / D^2 \text{ and } \alpha_0 = \text{arg} (l/2.D) \quad (1)$$

Where, I is the light intensity of the source (in Candela), D the distance light source/solar panel, and l the distance between LDR sensors (in cm).

With these conditions, received flux is given by [2]:

$$\begin{aligned} L_1 &= L_0 \cos (\Theta_0 - \alpha_e) \\ L_2 &= L_0 \cos (\alpha_e + \Theta_0) \end{aligned} \quad (2)$$

Nominal values in our small scale system are $D=1\text{m}$ and $l=10\text{cm}$ and $L_0=1000 \text{ lux}$.

3.2 Tracking system global modelling. The global equivalent mixed Spice schematic previously built in [2] is given in figure 6.

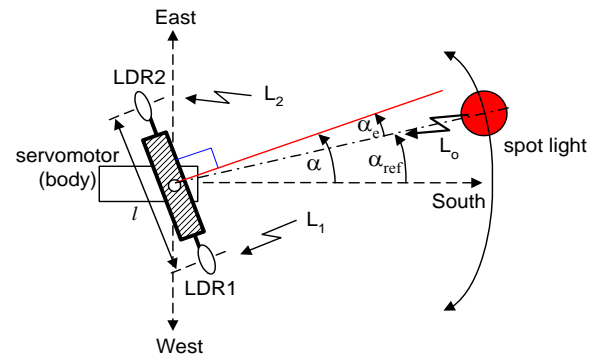


Figure 5: Reference angles (top view) modelling

3.3 LDR detailed modelling. LDR sensors are intrinsically nonlinear. Our commercial LDRs samples (VT90N) vary over 3 decades as a non-integer power of the received light (i.e. from $L^{-0.5}$ to $L^{-0.7}$), thus:

$$LDR(\Omega) = k \cdot \frac{1}{L^y} \quad (3)$$

(with $0.5 < y < 0.7$, and L in Lux)

The corresponding Spice modelling is given in figure 7. LDR, modelled by a Voltage Controlled Resistor block ("VCR"), is inserted in a resistor bridge supplied under +5V. Capacitor C4 represents the average time constant of the LDR as defined in [2].

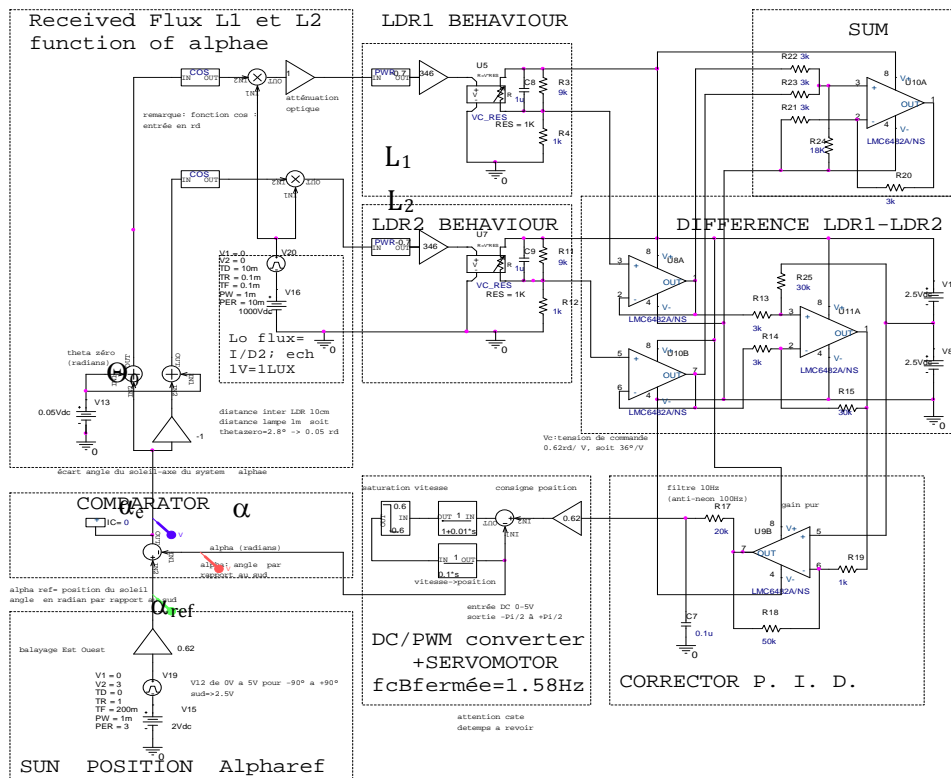


Figure 6: Global SPICE modelling

3.4 LDR detailed modelling. LDR sensors are intrinsically nonlinear. Our commercial LDRs samples (VT90N) vary over 3 decades as a non-integer power of the received light (i.e. from $L^{-0.5}$ to $L^{-0.7}$), thus:

$$LDR(\Omega) = k \cdot \frac{1}{L^y}$$

(3)

(with $0.5 < y < 0.7$, and L in Lux)

The corresponding Spice modelling is given in figure 7. LDR, modelled by a Voltage Controlled Resistor block (“VCR”), is inserted in a resistor bridge supplied under +5V. Capacitor C4 represents the average time constant of the LDR as defined in [2].

4. IDENTIFICATION OF IMPERFECTIONS

Since the tracking system is basically a feedback circuit, imperfections of active blocks are obviously greatly reduced. However, quality of sensors (which belong to the return loop) can impact directly the

performances of the system (accuracy, stability etc.).

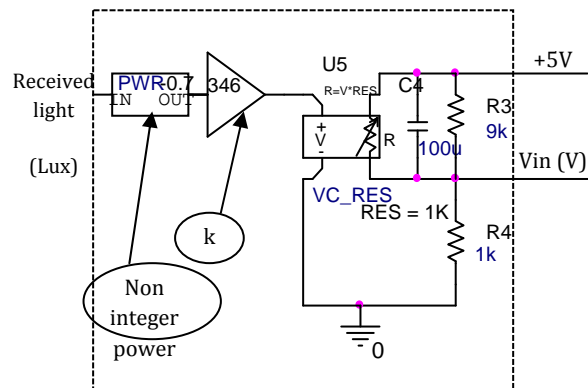


Figure 7: LDR generic modelling

In order to reduce this impact, the two LDR sensors were obviously sorted and a selection of two “similar” LDR was done. However, we estimate the residual global mismatching up to 10%.

Thus, it is important first to identify the different imperfections sources and to predict their effects and finally to suggest some possible compensations.



"HENRI COANDA"
AIR FORCE ACADEMY
ROMANIA



"GENERAL M.R. STEFANIK"
ARMED FORCES ACADEMY
SLOVAK REPUBLIC

INTERNATIONAL CONFERENCE of SCIENTIFIC PAPER
AFASES 2015
Brasov, 28-30 May 2015

The main imperfections identified are as follow.

- Intrinsic non linearity of the LDR
- Mismatching between LDRs:
 - Variation in k factor
 - Dispersion of the y exponent from -0.5 to -0.7
 - Dispersion of time response
 - Optical attenuation on LDR protection layer due to the dirt.
- LDRs ambient temperature variations

5. ANALYSIS OF LDR SENSOR'S NON LINEARITY

5.1. Impact of non-linearity. Non linearity leads to several consequences:

- A non-constant sensitivity over the full luminous flux range,
- A higher difficulty to match the two sensors response
- A possible instability depending on light level L_0 .

5.2. Non linearity SPICE simulations. Due to non-linearity, open loop gain depends on L_0 value. And the frequency response of the closed loop, with a parametric sweep for $L_0 = 10, 100, 1000$ and 10000 Lux is like indicated in figure 8. Gain in bandwidth is obviously close to 1, and a resonant frequency appears at high source intensity level.

6. ANALYSIS OF LDR SENSOR'S MISMATCHING

6.1 Impact of mismatching. Mismatching leads to several consequences:

- A possible permanent position angle error,
- Local instability.

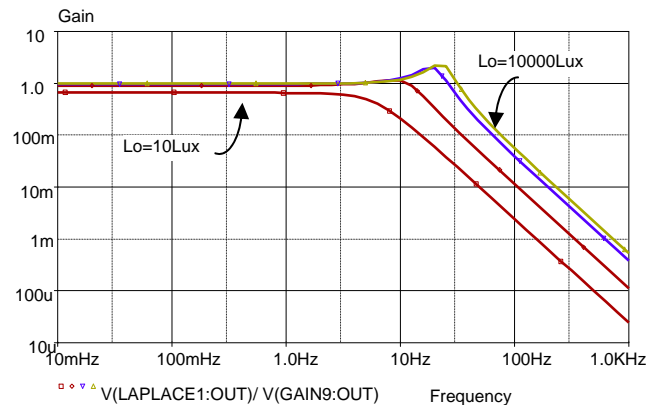


Figure 8: Closed loop gain

6.2 Impact of "k" factor

6.2.1 Analysis method

In a Log/log representation of LDR characteristic, varying k corresponds to a change of vertical offset (Cf. figure 9). A parametric sweep corresponding to a 10% variation on the LDR1 sensor is performed.

6.2.2 SPICE simulations

For these simulations, the system is initially pointed to south direction. A preliminary simulation is done as indicated hereafter:

- Tracking system in open loop. DC sweep from $L_0 = 10$ to 10000 Lux (full luminous range) with a parametric sweep of k value from 306 to 386 on LDR1 (Symmetric compared to the nominal value) to produces a voluntary mismatching.

Figure 9 shows the corresponding simulated behaviour of the LDR. Once LDR behavior checked, another simulation is run:

- a DC sweep from $L_0 = 10$ to 10000 Lux in closed loop with the same parametric sweep of k.

Using the «Spice performance analysis» option, once can extract the average error angle α_e vs. k (Cf. figure 10).

A variation of $\pm 11\%$ of k value around the nominal value leads to a huge error α_e of ± 1 rd (i.e. $\pm 57^\circ$).

6.3 Impact of y exponent

6.3.1 Analysis method

We perform a parametric sweep of exponent number y , in the “power block” ABM spice element. In Log/log representation of LDR characteristic, variation of power order y corresponds to a change in curve slope (cf. figure 11).

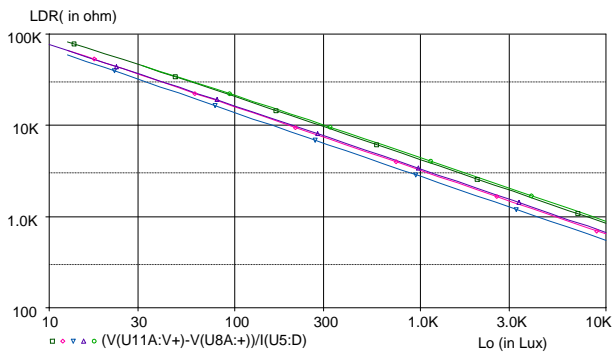


Figure 9: $LDR(\Omega) = f(L_0)$ Lux parametric analysis k

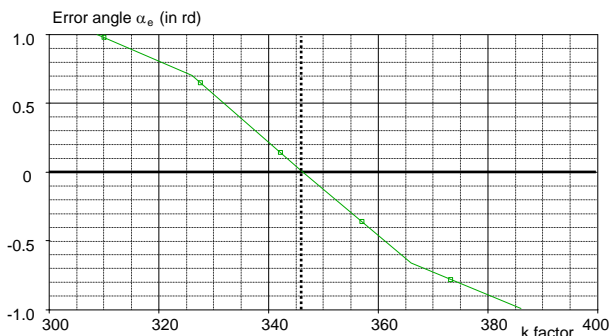


Figure 10: Error angle $\alpha_e = f(k)$

6.3.2 SPICE simulations

A first simulation is done as indicated hereafter:

- Tracking system in open loop. DC sweep from $L_0 = 10$ to 10000 Lux with a parametric sweep of exponent y of LDR1 from -0.65 to -0.75 (symmetric compared to the nominal value -0.7). Figure 11 shows the corresponding simulated behavior of the LDR.

Once LDR behavior checked, a second simulation is run:

- DC sweep from $L_0 = 10$ to 10000 Lux in closed loop with the same parametric sweep of y .

Using the «Spice performance analysis» option, one can obtain an average error angle

α_e around $L_0 = 300$ Lux. (as α_e depends on absolute value L_0).

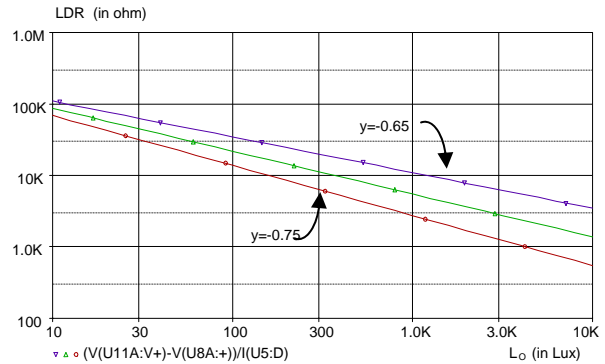


Figure 11: $LDR(\Omega) = f(L_0)$ Lux (parameter y)

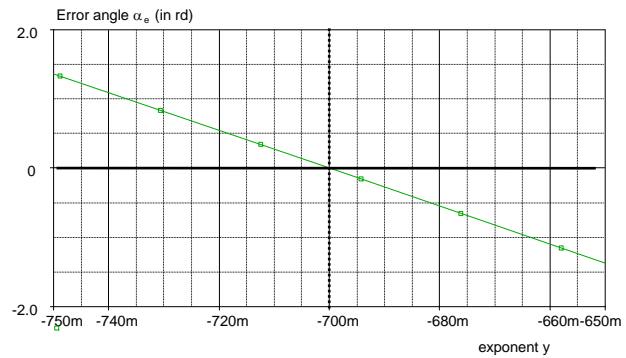


Figure 12: Error angle $\alpha_e = f(y)$ vs. y exponent

A +/-5% variation of y around -0.7, produces a huge deviation of angle error +/- 1 rd (i.e. 57°). The relative impact of y is greater than the one of k .

6.4 Impact of response time

6.4.1 Analysis method

A parametric sweep of 10% on capacitor value $C4$ is performed.

6.4.2 SPICE simulations

A mismatching on capacitor value does not have any impact in DC mode. But it may have an impact. Thus, the following transient analyses are performed:

- Response to a α_{ref} step pulse. The pulse characteristics are rise time 10ms, pulse width 4s, step of +/-1/2 rd around 0 (south position). $L_0 = 1000$ Lux, Figure 13 shows the response in closed loop, when capacitors are equal to 100μF and perfectly matched.

A 10% variation on capacitor value does not have significant effect. So, an extreme capacitor mismatching is simulated (100μF for



"HENRI COANDA"
AIR FORCE ACADEMY
ROMANIA



"GENERAL M.R. STEFANIK"
ARMED FORCES ACADEMY
SLOVAK REPUBLIC

INTERNATIONAL CONFERENCE of SCIENTIFIC PAPER
AFASES 2015
Brasov, 28-30 May 2015

LDR2 and 1 μ F LDR1) to check asymptotic behavior.

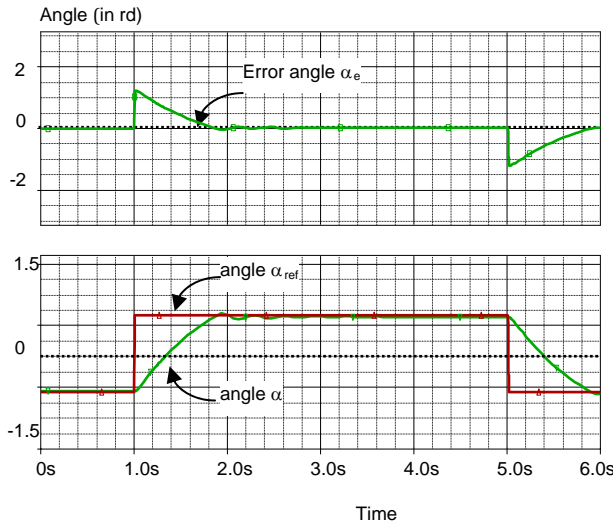


Figure 13: Transient simulations (C matched)

Figure 14 shows the response curve. The transient shape changes a little bit but the global behavior remains correct.

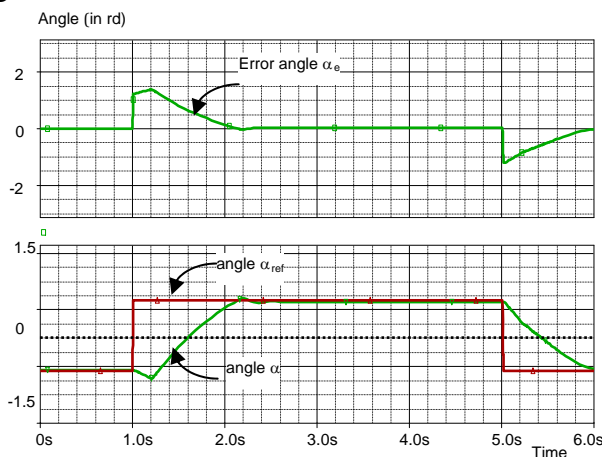


Figure 14: Transient simulations (C huge mismatch)

- Response to a 100Hz squared stimuli on L_0 : It represents the parasitic 100Hz flicker noise coming from fluorescent neon tubes in the room, during in door experimentation. The simulation conditions are rise time 0.1ms,

pulse width 1ms, period 10ms, nominal value $L_0=1000$ Lux, $\mu_{ref}=0$.

A 10% variation on capacitor value does not have significant effect. Like previously, the same extreme capacitor mismatching is simulated to check asymptotic behaviour.

Figure 15 shows the response curve. A permanent small error angle α_e (less than 4.5°) is observed.

Thus, the system is almost insensitive to this noise since mismatching between LDR time response remains small (less than 10%).

In fact, the previous simulations do not represent realistic phenomenon and should not be necessary for a real system, because all natural phenomenon are extremely slow: sun goes always in the same direction; there is no sudden movement of the sun or sudden change of light intensity in the Nature.

However, simulations were required to check reaction of the system since it works with "in door" conditions, which are different from reality.

6.5 Impact of optical attenuation

6.5.1 Modelling of optical attenuation.

A 0.9 attenuator SPICE element is placed in series on LDR1 received light input to produce voluntarily a difference in optical ways between LDR1 and LDR2.

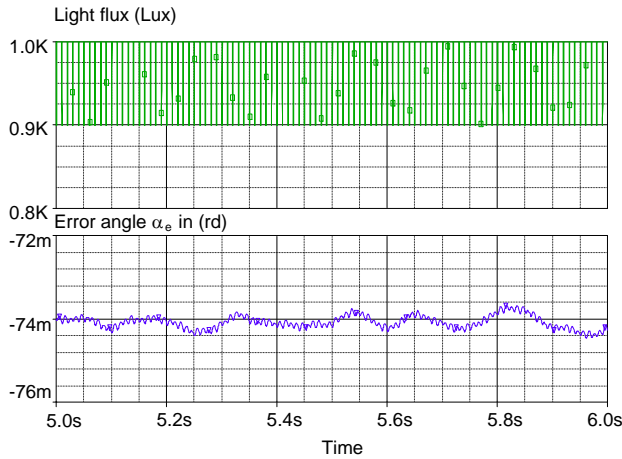


Figure 15: Transient simulations

6.5.2 SPICE simulations

These simulations investigate the static behavior in open loop, when submitting the system to a DC sweep of α angle from -90° to $+90^\circ$ (i.e. full rotation from East to West). The spot light is locked in south position ($\alpha_{ref} = 0^\circ$), $D=1m$ and $L_0=1000$ Lux.

As the distance between sensors is an important parameter, two cases have been tested:

- Distance between LDR sensors $l=10cm$

(i.e. $\Theta_0 \approx 2.8^\circ$) (Cf. figure 16).

- Distance between LDR sensors $l=60cm$

(i.e. $\Theta_0 \approx 18^\circ$) (Cf. figure 17).

Figure 16 shows the received light L_1 and L_2 vs. angle α . It can be read as follow:

L_1, L_2 reach their maximum values L_0 (here $=1000$ lux) when the spotlight is exactly in front of them (Respectively $\alpha_e = \Theta_0$ and $\alpha_e = -\Theta_0$). And they tend toward 0 when α reaches $\pm 90^\circ$ (Sunset or sunrise situation). When feedback loop operates normally, the system tends to make the two received lights flux, equal. This happens on figure 16 (resp. 17) at the intersection between the two curves L_1 and L_2 . Thus, the corresponding error angle can be deduced.

Here, we obtain $\alpha_e \approx 45^\circ$.

Vertical scale: received light in Lux

Green curve: L_1 (after optical attenuation $\times 0.9$)

Blue curve: L_2 (no attenuation)

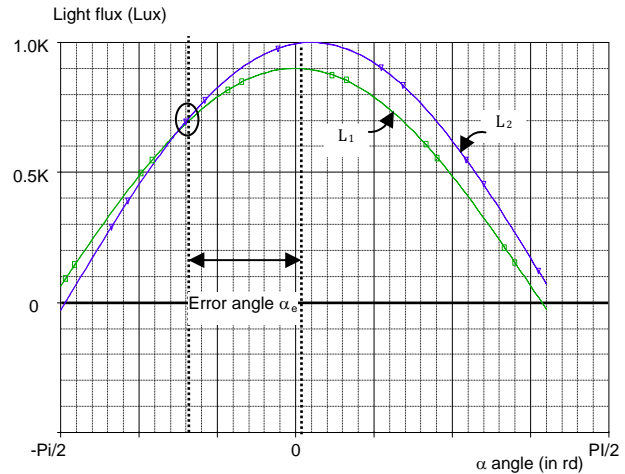


Figure 16: DC Sweep Simulations

Figure 17 shows also the received light L_1 and L_2 vs. angle α . Distance between sensors is 6 times greater than in figure 16 (i.e. 60cm). In this situation, error angle α_e is reduced to around 15° ; the more sensors are spaced, the less is the static angle error due to optical mismatching.

Vertical scale: received light in Lux

- Red curve: L_1 (before attenuation)

- Green curve: L_1 (after optical attenuation $\times 0.9$)

- Blue curve: L_2

6.6 Temperature impact

The ambient temperature changes from morning to afternoon. Unfortunately, LDRs are sensitive to temperature [8]: the LDR resistance value decreases as the temperature rises.

The relationship between temperature and resistance was not completely investigated but it appears that the resistance of an LDR is a function of both light flux and temperature.

For our “in door” application with a spot light of 75 to 100W, 1meter far, and distance between sensor 10cm, this is not really a problem. However, for outdoor uses, when the component is oriented towards the sun, the LDR resistance becomes very low, and the effects of temperature variation could appear more significant.



"HENRI COANDA"
AIR FORCE ACADEMY
ROMANIA



"GENERAL M.R. STEFANIK"
ARMED FORCES ACADEMY
SLOVAK REPUBLIC

INTERNATIONAL CONFERENCE of SCIENTIFIC PAPER
AFASES 2015
Brasov, 28-30 May 2015

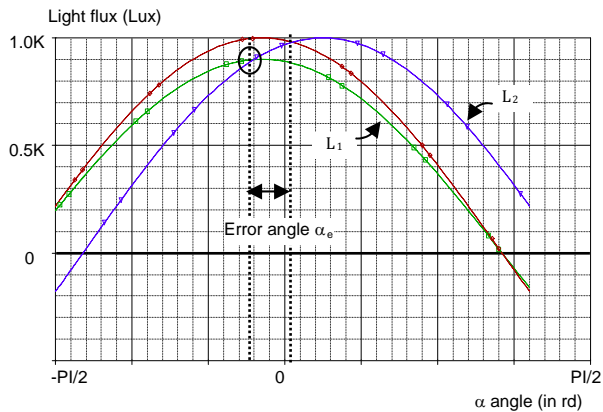


Figure 17: DC sweep Simulations

7. EXPERIMENTS

It is difficult, from experimental point of view, to reproduce exactly the simulated mismatching because it could require a lot of mismatched LDR and many repetitive tests.

We only performed some tests with a few "no sorted" LDRs. Due to the test bench, a fine measurement of accuracy is difficult to obtain. However, when LDR are mismatched, the main tendencies and order of magnitude of error angle α_e predicted by simulation are experimentally checked.

When the two LDR are matched, the system tracks correctly the light source with accuracy better than 5° , which is enough for demonstrating the theoretical principle of tracking and for public exhibition purposes.

8. DISCUSSION AND COMMENTS

Angle accuracy of the system is affected by all the imperfections. Among the four parameters, non-integer power exponent y is the most influent. Instability risk comes from the nonlinear intrinsic behavior of LDR. Distance l between LDR sensors is an

important factor: the more they are spaced, the less is the static angle error.

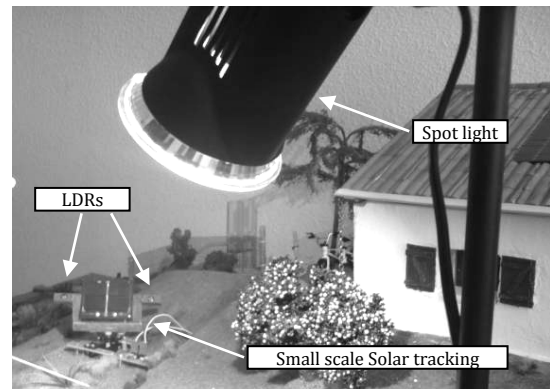


Figure 18: Practical test

The small scale solar tracking system will operate whatever the situation, but with a more or less important static permanent error. From simulations, a maximum error of 5° requires a global matching better than 1% between LDR sensors.

As perfect matching between sensors is never possible, some improvements can help to reduce the error. Two kind of improvement can be investigated. Whatever the strategy, a preliminary strong sorting of LDR sensors is required. Then, a linearization circuit can be added, if necessary. It can be done in two ways:

- by using a micro controller with a tabulated conversion table (a new design is already planned)
- by using analogue circuits with voltage dependant gain circuit (diode or multiplier) and OP amps for offset and gain adjustments.

9. CONCLUSION

A small scale solar tracking system was designed and an equivalent mixed modelling was presented. Effects and impacts of major imperfections were studied and quantified.

Possible improvements to compensate imperfections have been suggested. However, the presented system is not mass produced; it is only a unique experimental device. Thus, there was no need to include such improvements in the present design till now. The tracking system is now installed in on our small scale greenhouse modelling. And some exhibitions have been planned for general public sensitizing in the near future.

REFERENCES

- [1] Ph. Dondon- P. Cassagne- M. Feugas- C.A. Bulucea- D.Rosca-V. Dondon- R. Charlet de Sauvage “*Concrete experience of collaboration between secondary school and university in a sustainable development project: design of a realistic small scale house to study electronic and thermal aspect of energy management.*” WSEAS Transactions on ENVIRONMENT and DEVELOPMENT Issue 10, Vol 7, oct 2011, ISSN: 1790-5079 p 225-235
- [2] Ph. Dondon, L. Miron « *Modelling and design of a small scale solar tracking system -Application to a green house model-* » WSEAS Transactions on ENVIRONMENT and DEVELOPMENT Issue 10, Vol 7, oct 2013, ISSN: 1790-5079 p 225-235
- [3] « *Choix d’un suiveur solaire* » http://www.energieplus-lesite.be/energieplus/page_16690.htm?reload
- [4] <http://www.exosun.fr/index.php>
- [5] T. Bendib, B. Barkat, F. Djeflal, N. Hamia et A. Nidhal « *Commande automatique d’un système de poursuite solaire à deux axes à base d’un microcontrôleur PIC16F84A* » Revue des Energies Renouvelables Vol. 11 N°4 (2008) 523 – 532
- [6] C.S. Chin, A. Babu, W. McBride. « *Design, Modelling and testing of a Standalone Single-Axis Active Solar Tracker using MATLAB/Simulink* » Renewable Energy journal, 01/2011; ISSN 0960-1481
- [7] PC Control Ltd web site: http://www.pc-control.co.uk/howto_tracksun.htm
- [8] Brighton Webs Ltd. web site: http://www.brighton-webs.co.uk/electronics/light_dependent_resitor.htm